A Close Examination of Under-Actuated Attitude Control Subsystem Design for Future Satellite Missions' Life Extension

Quang M. Lam[1, a)] and Itzhak Barkana[2, b)]

[1] *Jesplsoft*, *Fairfax, VA*, USA
[2] BARKANA *Consulting*, Ramat Hasharon, ISRAEL

[a)]Corresponding author: quang.lam@Jesplsoft.com
[b)]ibarkana@gmail.com

Abstract. Satellite mission life, maintained and prolonged beyond its typical norm of their expectancy, are primarily dictated by the state of health of its Reaction Wheel Assembly (RWA), especially for commercial GEO satellites since torquer bars is no longer applicable while thrusters assistant is unacceptable due to pointing accuracy impact during jet firing. The RWA is the primary set of actuators (as compared to thrusters for orbit maintenance and maneuvering) mainly responsible for the satellite mission for accurately and precisely pointing its payloads to the right targets to conduct its mission operations. The RWA consists of either a set of four in pyramid or three in orthogonal mainly responsible to achieve accurate and precise pointing of the satellite payloads towards the desired targets. Future space missions will be required to achieve much longer lives than has been deemed acceptable during the last three decades. Driven by customers' demands/goals and competitive market have challenged Attitude Control Subsystems (ACS) engineers to develop better ACS algorithms to address such an emerging need. There are two main directions to design satellite's under-actuated control subsystem: (1) Attitude Feedback with Zero Momentum Principle and (2) Attitude Control by Angular Velocity Tracking via Small Time Local Controllability concept. Successful applications of these control laws have been largely demonstrated via simulation for the rest to rest case. Limited accuracy and oscillatory behaviors are observed in three axes for non-zero wheel momentum while realistic loss of a wheel scenario (i.e., fully actuated to under-actuated) has not been closely examined! This study revisits the under-actuated control design with detailed set ups of multiple scenarios reflecting real life operating conditions which have put current under-actuated control laws mentioned earlier into a re-evaluation mode since rest to rest case is not adequate to truly represent an on orbit failure of a single wheel. The study is intended to facilitate the ACS community to further develop a more practical under-actuated control law and present a path to extend these current thinking to address a more realistic reconfigurable ACS subject to a dynamic transition from a 3 RWs mode to 2 RWs mode.

I. INTRODUCTION

Self-Repairing or Reconfigurable Flight Control System (FCS) design subject to loss of control surfaces (actuators) and/or sensors due to component aging or battle damage is the well-known topic and in fact considered as a requirement for a certain military aircraft. For aircraft or any flight vehicle operating within the atmospheric domain, the concept of aerodynamic redundancy can be exploited to generate a replacement of a loss thrust vector by using the remaining control surfaces. For spacecraft, aerodynamic redundancy concept is no longer applicable, and the loss of critical control actuators like Reaction Wheel Assembly (RWA), which normally reflects a four wheels mounted in a pyramid configuration to offer redundant 3 axis control stabilization and to enhance its overall torque capacity, will result in a loss of pointing control accuracy (i.e., pointing control accuracy degradation, i.e., no longer meeting the original pointing requirement and operating right outside the envelope of the control pointing budget) and for some case, totally lose its stabilization capability.

The need to fly a commercial communication satellite and US Government Space Programs using a RWA under severe degraded operating conditions of the individual wheels within the RWA has been investigated during the past 10 years, especially for the under-actuated control situation (i.e., only two remaining operational wheels while need to stabilize and control the spacecraft in three axes). Commercial Geostationary Earth Orbit (GEO) missions, has recently been aimed at reaching its 20 years life of services or beyond from a typical normal life of 15 tears. This goal, driven by customers' demand and competitive market, has challenged Attitude Control Subsystems (ACS) engineers to develop adequate ACS algorithms to accommodate this extended life of services in the presence of limited and aging hardware components (i.e., ACS sensors and actuators).

Recently, the National Aeronautics and Space Administration (NASA) is seeking to obtain information on innovative approaches for spacecraft hybrid attitude control that employ mixed-actuator combinations of two reaction wheels and reaction control thrusters. Specifically NASA is seeking innovative hybrid attitude control approaches for the distressed Kepler spacecraft which has suffered performance anomalies with two of its four-reaction wheel attitude control actuators. NASA is interested in identifying potential organizations that are capable of generating innovative spacecraft hybrid attitude control approaches. The main research interest is to identify a credible and low risk hybrid intelligent control approach, timely mature them as technology insertion to support the Kepler Project Office. The main goal is to use such an under-actuated control technology to continue its use of the Kepler observatory's remaining functional capabilities to accomplish potentially new and different scientific objectives. In addition, NASA is also interested in identifying those hybrid control approaches that will enable the most compelling new science observations envisioned for a 'repurposed' Kepler science mission.

In this paper, we examine the loss of two RWAs out of three RWAs mounted in an orthogonal configuration to assess the true under-actuated control arena for space missions using a combination of direct adaptive control [1] as a robustness enforcer and/or assistant and Small Time Local Controllability (STLC) concept [2] as primary means of "spreading" the two remaining wheels' torques to three axes control. Our key design innovations are summarized as follows: (1) extending the STLC design principle to a practical operating condition to demonstrate its practical usefulness and state of practice capability for a real mission servicing as ACS software insertion and (2) demonstrate its robust and stabilization capability with two remaining wheels while not requiring any external control actuator help from thrusters. STLC concept has been demonstrated as the primary means to turn the under-actuated control condition into a less severe control operating condition by using the Angular Velocity Tracking to regain the three axes control stabilization (see [2] & [3] and their references for the design history). Most of the performance evaluations were conducted using benign starting conditions. Those include (1) starting the simulation with a loss of the 3^{rd} wheel and initial conditions are less severe; (2) initializing the spacecraft small initial angular rate magnitudes when start the two RWs simulation for the analysis; (3) only examine the loss of the 3^{rd} (yaw) wheel only (i.e., loss of RWs 1 or 2 will not be trivially solved using the fundamental STLC concept); (4) spacecraft inertia matrix is fully decoupled (i.e., only diagonal elements are non-zero); to name a few. In addition, successful applications of STLC to those investigations have been largely demonstrated via simulation for the *rest to rest case* (i.e., zero body angular rates and zero wheel momentum from the starting of the simulation.) Limited accuracy and oscillatory behaviors are observed in three axes for non-zero wheel momentum while realistic loss of a wheel scenario (from a fully actuated 3 wheels down to 2 wheels in 'pseudo' real time dynamic transition) has not been closely examined! Figure 1 describes the fundamental control challenges of a spacecraft in an under-actuated control situation.

This study revisits the under-actuated control design with detailed set ups of multiple scenarios reflecting real life operating conditions which have put current under-actuated control laws mentioned earlier into a re-evaluation mode since rest to rest case is not adequate to truly represent an on orbit failure of a single wheel (that put the satellite into an under-actuated control situation.) The study is intended to facilitate the Satellite ACS community to further develop a more practical under-actuated control law and present a practical control solution using a combination of STLC and Direct Adaptive Control (DAC) (also known as Simple Adaptive Control, SAC) for consideration as technology insertion. The study also discusses paths to extend the current specific design of the loss of the 3^{rd} wheel to a more generic solution with the loss of any single wheel in three axes (rather than just the 3^{rd} yaw RW only!)

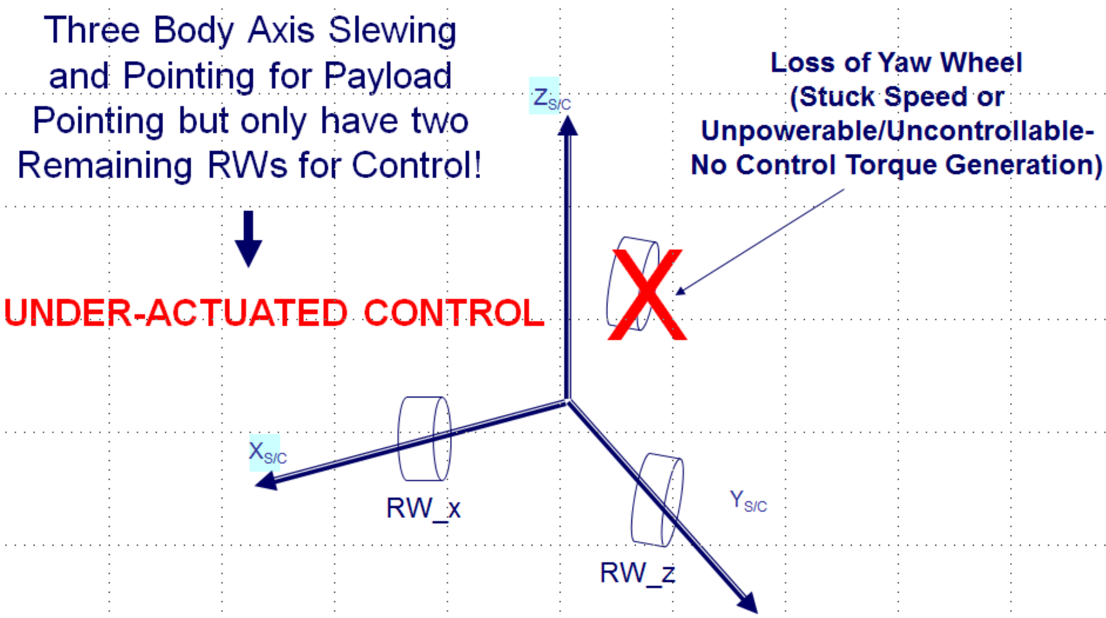

II. DIRECT ADAPTIVE CONTROL AND STLC CONTROL LAW DESCRIPTION

A. Direct Adaptive Control Algorithms

The Direct Adaptive Control Law developed in [1] for a four RWs mounted in a pyramid configuration control is leveraged here to assist the STLC dealing with the actual dynamic situation of three operational RWs down to 2RWs and successfully accomplish the under-actuated control condition. The DAC algorithm is re-used here for the sake of self-contained and convenient for readers to cross-reference it if needed

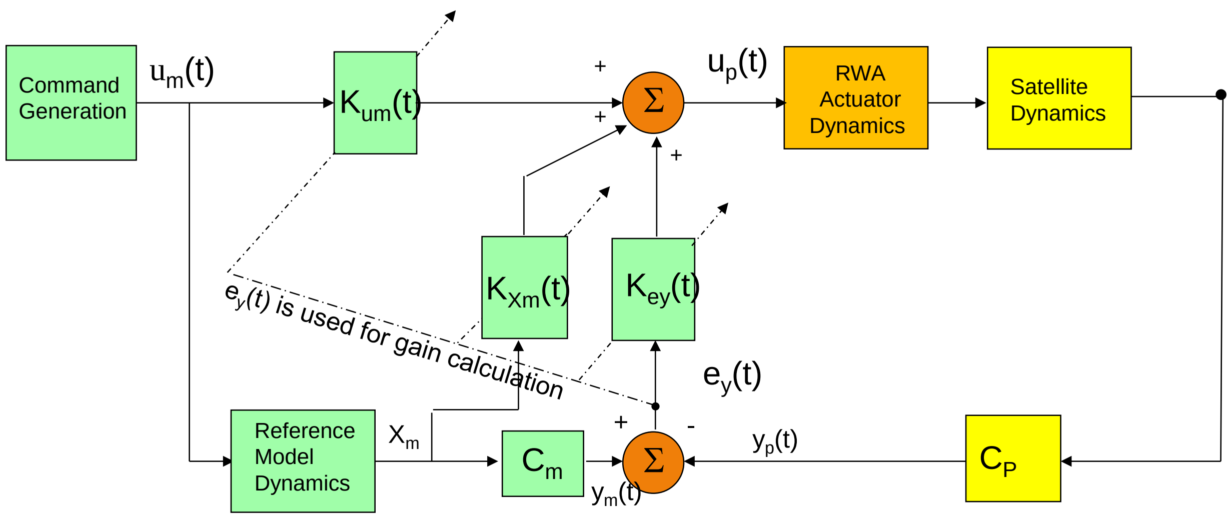

Figure 2: Direct Adaptive Control (DAC) or Model Reference Adaptive Control Architecture

With respect to Figure 2 for a DAC control configuration, define the feed-forward control torque as

$$u_m = [u_{mx} \quad u_{my} \quad u_{mz}]^T \tag{2.A.1}$$

The reference model dynamics are nonlinear dynamics which are generated via dynamic propagation using the dynamic model with rate command as the signal generator. They are designed to produce a desired dynamic state vector x_m consisting of desired angular rate and desired quaternion attitude information, respectively as follows:

$$x_m = [q_e \mid \omega_m]^T = [q_{ex} \quad q_{ey} \quad q_{ez} \mid \omega_{mx} \quad \omega_{my} \quad \omega_{mz}]^T \tag{2.A.2}$$

Note that since direct adaptive control is employed here, a set of explicit linearized reference model dynamics is not required to be augmented with the plant dynamics in order to design the whole controller as the traditional explicit model-following/LQR design technique. In other words, the direct adaptive control gain generation scheme requires only the existence of the [um | xm] of the reference model dynamics in order to compute its fully-coupled gain matrix; nevertheless, it does not care much about the structure as well as the dynamics of the reference model as required by the traditional EMF/LQR[1].

The nonlinear plant dynamics is the Euler moment equation with the plant dynamics state vector is structured as follows:

$$x_p(t) = [q \mid \omega]^T = [q_x \quad q_y \quad q_z \mid \omega_x \quad \omega_y \quad \omega_z]^T \qquad (2.A.3)$$

where q_i and ω_i are the spacecraft's measured quaternion attitude and the measured angular body rate, respectively. The complete direct adaptive control gain structure is computed using the design rationale of [4]:

$$K(t) = [K_{um}(t) \mid K_{xm}(t) \mid K_{ey}(t)]^T \qquad (2.A.4)$$

where each respective gain block is described as follows:

$$K_{um}(t) = K^I_{um}(t) + K^P_{um}(t) \qquad (2.A.5)$$

$$K_{Xm}(t) = K^I_{Xm}(t) + K^P_{Xm}(t) \qquad (2.A.6)$$

$$K_{ey}(t) = K^I_{ey}(t) + K^P_{ey}(t) \qquad (2.A.7)$$

In other words, each adaptive gain block expressed in equations (2.5) to (2.7) consists of two main components: integral and proportional (i.e., $K^i(t)$ and $K^p(t)$).

To further describe the detailed implementation of each gain block specifically developed for this study, we break each adaptive gain block into a three axis control (i.e., x, y, and z components) per signal level as follows:

$$K_p(t) = e_y(t) r^T(t) \Gamma_p \qquad (2.A.8)$$

$$\dot{K}_I(t) = e_y(t) r^T(t) \Gamma_I - \sigma K_I(t) \qquad (2.A.9)$$

where

$$e_y(t) = x_m(t) - x_p(t) = [q_e(t) \mid \omega_e(t)]^T \qquad (2.A.10)$$

and

$$r(t) = [u_m(t) \quad x_m(t) \quad e_y(t)]^T \qquad (2.A.11)$$

Note that the quaternion error is dynamically derived using quaternion multiplication rather than a pure straight subtraction.

From the symbolic expression of (2.8) and (2.9) with a 3 axis control block per signal level, we have each adaptive gain block computed as follows:

$$K_{pum}(t) = [K_{pum\_att}(t) \mid K_{pum\_rate}(t)] = [q_e(t) u_m^T(t) \Gamma_{pqe} \mid \omega_e(t) u_m^T(t) \Gamma_{p\omega e}] \qquad (2.A.12)$$

$$K_{Ium}(t) = [K_{Ium\_att}(t) \mid K_{Ium\_rate}(t)] = [q_e(t) u_m^T(t) \Gamma_{Iqe} \mid \omega_e(t) u_m^T(t) \Gamma_{I\omega e}] \qquad (2.A.13)$$

The adaptive gain for the $x_m(t)$ will have four individual blocks due to the expansion of two 3-axis control vectors for attitude and rate, respectively, for both command and feedback errors:

$$K_{pxm}(t) = [K_{pxm\_att}(t) \mid K_{pxm\_rate}(t)] = [q_e(t) x_m^T(t) \Gamma_{pqe} \mid \omega_e(t) x_m^T(t) \Gamma_{p\omega e}] \qquad (2.A.14)$$

$$K_{pxm}(t) = [q_e(t) q_m^T(t) \Gamma_{pq} \mid q_e(t) \omega_m^T(t) \Gamma_{pq\omega} \mid \omega_e(t) q_m^T(t) \Gamma_{p\omega q} \mid \omega_e(t) \omega_m^T(t) \Gamma_{p\omega}] \qquad (2.A.15)$$

Similarly, the integral portion has the following expanded structure of four individual blocks due to its two 3-axis vectors explained in [1]:

$$K_{Ixm}(t) = [q_e(t) q_m^T(t) \Gamma_{Iq} \mid q_e(t) \omega_m^T(t) \Gamma_{Iq\omega} \mid \omega_e(t) q_m^T(t) \Gamma_{I\omega q} \mid \omega_e(t) \omega_m^T(t) \Gamma_{I\omega}] \qquad (2.A.16)$$

Likewise, the $K_{Pey}(t)$ and $K_{Iey}(t)$ will take a similar structure of equation (2.13) and (2.14) since it contains two 3-axis vectors of attitude and rate, respectively:

$$K_{Pey}(t) = [q_e(t) q_e^T(t) \Gamma_{pqe} \mid q_e(t) \omega_e^T(t) \Gamma_{pq\omega}] \qquad (2.A.17)$$

$$K_{Iey}(t) = [q_e(t) q_m^T(t) \Gamma_{Iq} \mid q_e(t) \omega_m^T(t) \Gamma_{Iq\omega}] \qquad (2.A.18)$$

Note that the DAC algorithm described in this section is able to provide a robust control capability on its own to a satellite's full ACS problem evaluated at the complexity of a full nonlinear dynamic of the satellite pointing control problem [1]. In this application, it is being used on a per axis basis as an assistant (see Figure 5 for its appropriate insertion and implementation) to the STLC to accomplish the under-actuated control problem.

B. STLC Control Algorithms

The detailed derivation of the STLC control law can be referred back to [2] and [3]. Its performance validity for three axis maneuvering with two RWs is built on the zero-momentum constraint principle. Since the zero-momentum constraint yields an algebraic relation between the wheel speeds and angular velocities, the wheel speeds can be designed directly as a function of attitude orientation to re-orientate the spacecraft. This may be suitable for applications without any angular velocity information, but requires perfect zero-momentum condition. Therefore, the kinematic and dynamic equations of attitude motion are considered in the following controller design. Using the exact restricted condition of the STLC for the loss of the 3rd RW and the yaw angular rate continues remaining zero [3] (eq. (4) leading to eqs. (10) to (12)), the 3 axis stabilization control under two remaining RWs is reduced to the following two equations:

$$\begin{pmatrix} q_0 \\ q_1 \\ q_2 \\ q_3 \end{pmatrix} = \frac{1}{2} \begin{pmatrix} -q_1 & -q_2 \\ q_0 & -q_3 \\ q_3 & q_0 \\ -q_2 & q_1 \end{pmatrix} \begin{pmatrix} \omega_1 \\ \omega_2 \end{pmatrix} \qquad (2.B\text{-}1)$$

Note: The vector part is $[q_1 \mid q_2 \mid q_3]$

$$\begin{bmatrix} I_{11}\omega_1 \\ I_{22}\omega_2 \\ 0 \end{bmatrix} = \begin{bmatrix} u_1 \\ u_2 \\ 0 \end{bmatrix} \qquad (2.B\text{-}2)$$

The two RWs control actions $u=[u_1|u_2]^T$ is computed based on the attitude feedback of roll and pitch attitude (i.e., q_1 and q_2) as follows,

$$\begin{bmatrix} u_{1cmd} \\ u_{2cmd} \end{bmatrix} = -k \begin{bmatrix} q_1 \\ q_2 \end{bmatrix} + 2g \begin{bmatrix} \Delta_2 \\ -\Delta_1 \end{bmatrix} \qquad (2.B\text{-}3)$$

with Δ_i computed as follows,

$$\Delta_i = \frac{q_i q_3}{q_1^2 + q_2^2} \qquad (2.B\text{-}4)$$

Note: The 3rd axis control with only two control torques delivered by two remaining RWs can be intuitively seen by the numerator of the equation (2.B-4). This is shown by the coupling of the 3rd axis attitude q_3 being "fed-back" into the Δ_i, i=1,2 which is being used by the two remaining active RW_1 and RW_2.

The above attitude feedback (via quaternion) control law is being implemented into Simulink as shown in Figure 3 below with the intended ground out of the 3rd axis angular rate component in the bottom of the figure.

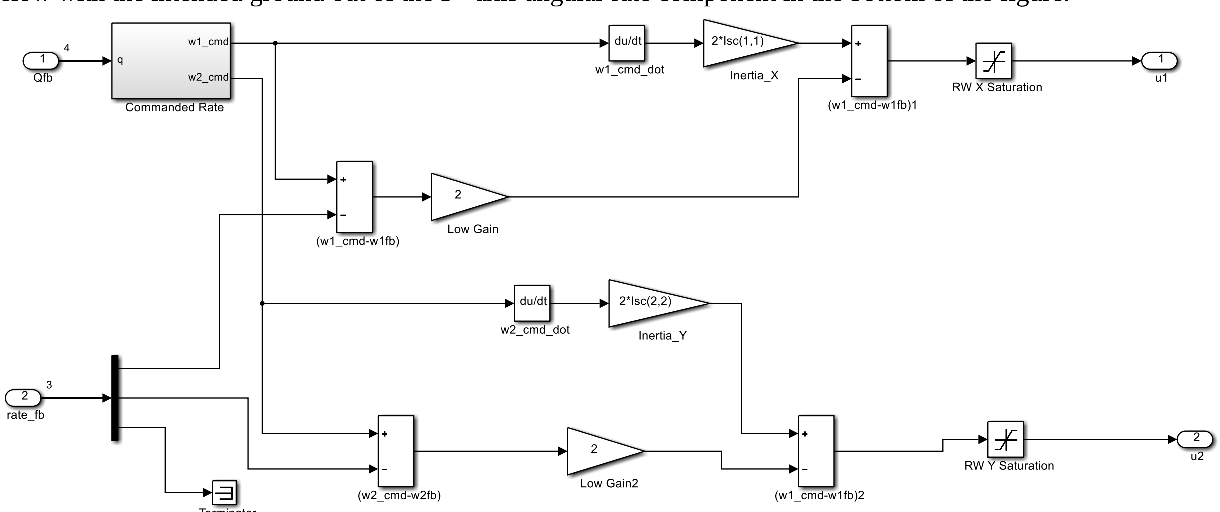

Figure 3: Two Reaction Wheel Control Law Implementation Via Attitude Quaternion Feedback

The Δ_i quantity (of equation (2.B-4)) within the STLC is being "clamped" by an amplitude saturation function defined as below:

$$sat_q(\Delta_i) = \begin{cases} sign(q_3)\ if q_1 = q_2 = 0 \\ \Delta_i\ if\ abs(\Delta_i) \leq 1 \\ sign(\Delta_i)\ if abs(\Delta_i) \geq 1 \end{cases} \qquad (2.B\text{-}5)$$

where

$$sign(x) = \begin{cases} 1 & if \quad x > 0 \\ 0 & if \quad x = 0 \\ -1 & if \quad x < 0 \end{cases} \qquad (2.B\text{-}5)$$

The full blown STLC control law at the next level is shown in Figure 4.

III. PERFORMANCE EVALUATION

A. Simple Check on the STLC Control Law Implementation & Its Validity

This section is a STLC control law design implementation check using the loss of the yaw RW (3rd axis) control design defined and developed in [3] (see Section 4, Global Feedback Control). The 3rd RW (Yaw Wheel) Torque and Momentum Loss are shown in Figures 5 and 6, respectively. The stable performance and accurate ACS command tracking described in Figures 8 and 9 is the validation of the STLC implementation.

Remarks: Note that under this STLC design (summarized in Section 2, Subsection B of this paper), several key items are brought to your attention as main motivation for our investigation conducted in this paper. They are:

- There are no realistic satellite torque disturbances employed in the analysis of previous investigators
- The STLC control law developed using the loss of the 3rd RW (in the yaw axis) is not universal and can't be applied or generalized to address the loss of any other individual RW for the other two axes (i.e., loss of 1st RW in the Roll Axis or 2nd RW in the pitch axis)
- The STLC control law described in [2] and [3] are not fully capable of addressing automatic RW failures detection and adaptive reconfigurable control action generation in real time.

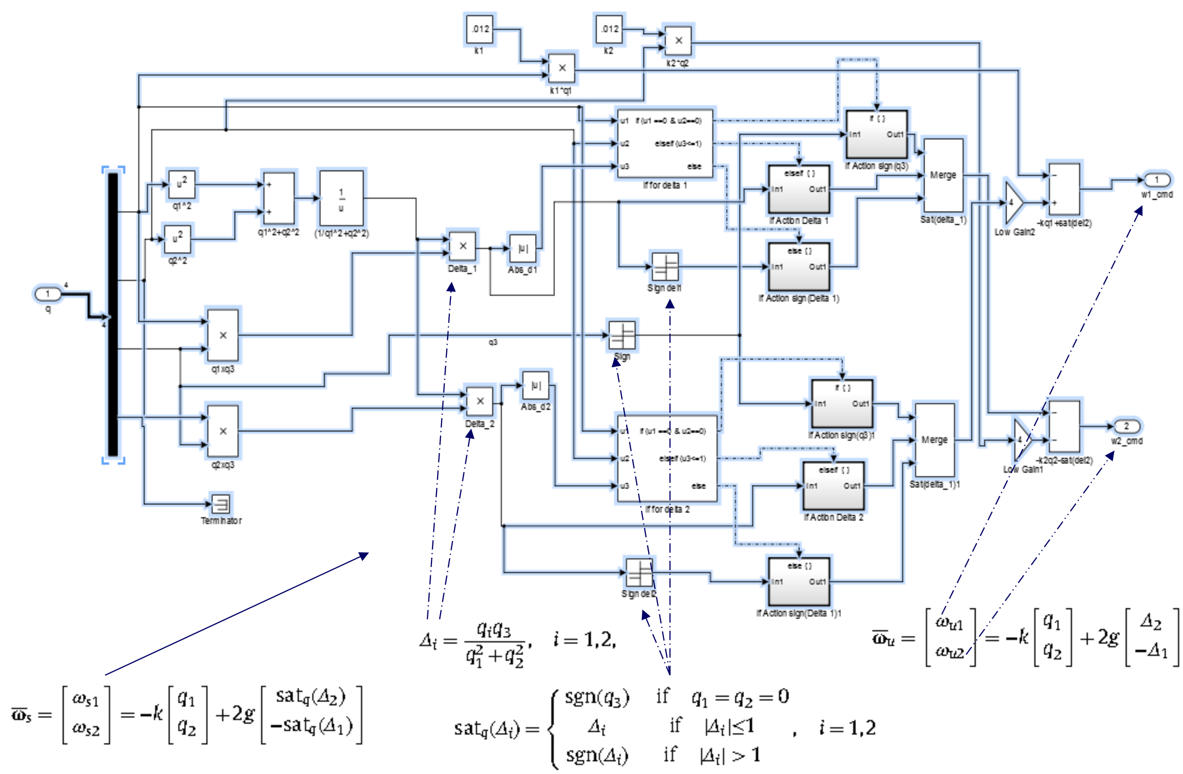

Figure 4: Full Blown STLC Control Law for RW_1 and RW_2 Implemented in Simulink

B. Practical Evaluation With Dynamic Transition from 3RWs Down to 2RWs Using the STLC Alone

The nice performance of the STLC control law for the loss of the 3rd RW (Yaw Wheel) shown in Case A under "rest to rest" condition and nice start from the get go with benign initial conditions is now being put to test for a more realistic operating condition. That realistic condition is the random transition from a normal 3RWs down to 2RWs due to a sudden loss of the 3rd RW. Under this situation, the angular rate vector will have non-zero value for all of its components and other state vectors (e.g., attitude, acceleration, stochastic disturbances, etc) will have a drastic change due to such a sudden loss of the 3rd RW.

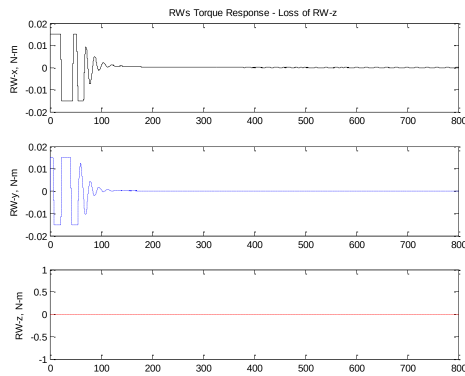

Figure 5: Loss of RW3 (Yaw Wheel) Right from the Get Go (at the Beginning of the Sim)

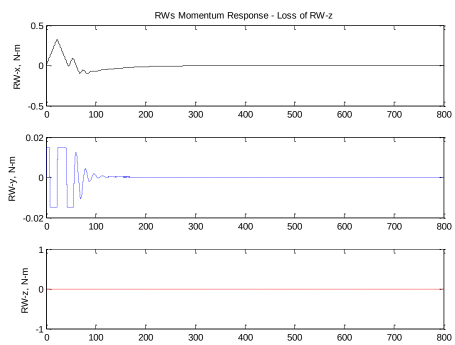

Figure 6: RW Momentum Response

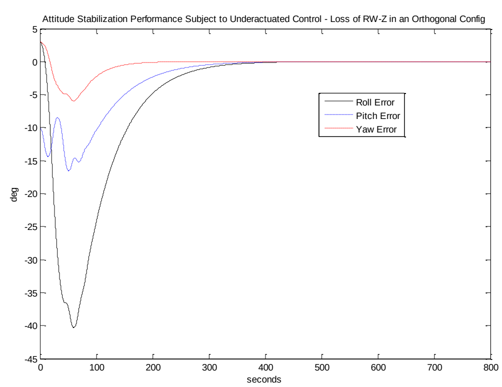

Figure 7: Performance Check of STLC Control Law Alone Under Loss of the Yaw RW (in the 3rd Axis)

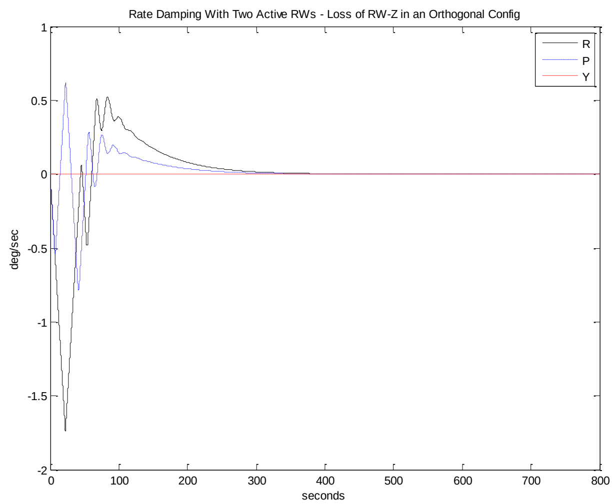

Figure 8: Rate Damping Ability in all Three Axes with Only RW1 and RW2

B.1: STLC Performance Subject to Disturbances

As predicted, under this realistic failure situation the STLC control laws fail to stabilize the spacecraft in all axes. Figure 10 shows the STLC weakness for a mild disturbance introduced to the spacecraft system. Its stabilization in three axes are being compromised with some level of accuracy being degraded.

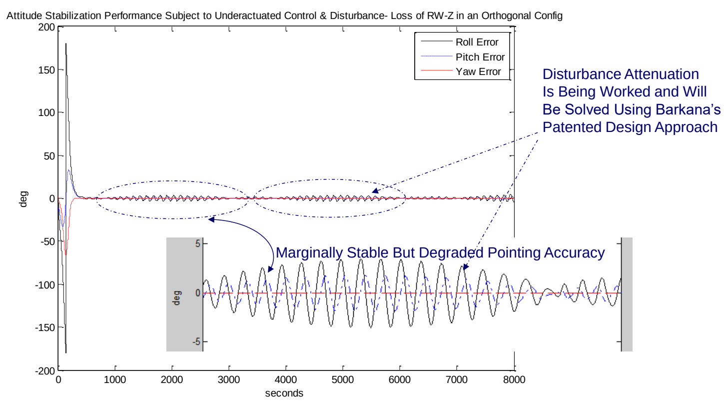

Figure 9: Degraded Attitude Performance of the STLC Subject to Disturbances

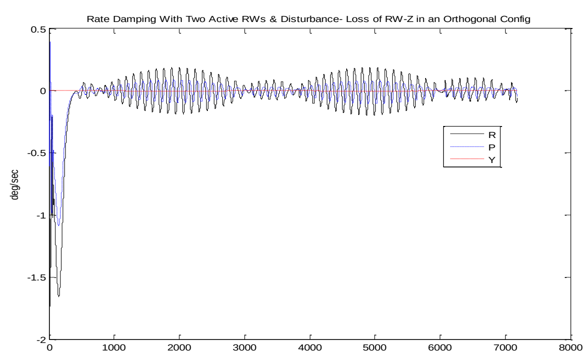

Figure 10: Degraded Rate Performance of the STLC Subject to Disturbances

B.2: STLC Performance Subject to a Random Loss of Yaw RW from a 3 Operational RWs

This scenario is illustrated in Figure 12 using the RWs torque profiles. The yaw wheel is out at the mark of the 180 seconds. This dynamic transition from 3RWs down to 2RWs has impacted the spacecraft stabilization and pointing in bot attitude and rate as shown in Figures 13 and 14, respectively.

C. Robust Performance of Both DAC and STLC to take Care of Realistic Operating Condition (3RWs down to 2RWs in Real Time)

The severe performance degradation of the STLC subject to the realistic 3RWs down to 2RWs during a normal operating condition shown in Section B is now treated under the addition of the DAC or SAC control law as implemented in Figure 5. With this STLC-DAC augmented configuration, the poor performance of the STLC control law alone is now being assisted by the DAC continuous actions. The DAC actions as an assistant have dramatically helped the STLC to regain its under-actuated control performance as its original developers have projected. Figures 15 to 18 demonstrate the performance effectiveness of the proposed DAC-STLC control laws. Its attitude pointing accuracy and rate damping performances have been nicely restored.

IV. CONCLUDING REMARKS

A closer examination of the satellite under-actuated control using RW actuators only (i.e., no thruster assistant action) is conducted. Realistic operating conditions and RW failure modes for individual RW are examined and accounted for in this investigation. Benign operating condition and theoretical design expectation of the promising STLC control law is validated. STLC control law has been determined to work well as under-actuated control law under mild operating conditions (i.e., no disturbances and no dynamic transition from 3RWs to 2RWs.) We injected realistic operating conditions to closely examine the STLC control law for its under-actuated control capability role and observe that STLC control law alone is not capable of handling disturbance torque or practical loss of a single wheel mimicking a practical dynamic transition from 3RWs down to 2RWs in real time. The *Simple Adaptive Control (SAC)* [5] or Direct Adaptive Control (DAC) is then added in and implemented in an augmented fashion *as an assistant to the STLC control law* to provide needed actions in an adaptive reconfigurable control manner, and with this proposed STLC/SAC control implementation a true under-actuated control performance is observed for its potential contribution to future space missions in the context of robust

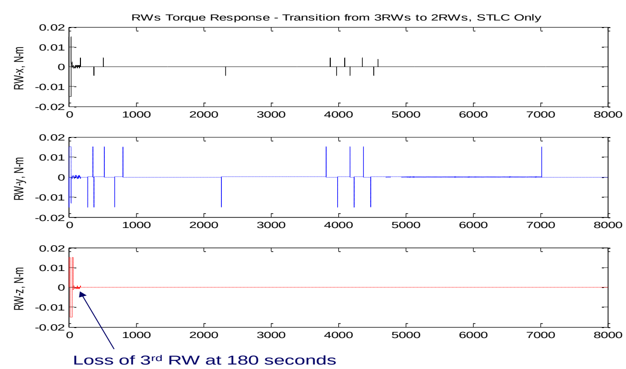

Figure 11: RWs Torques Profile With a Loss of the 3rd RW at 180 Seconds

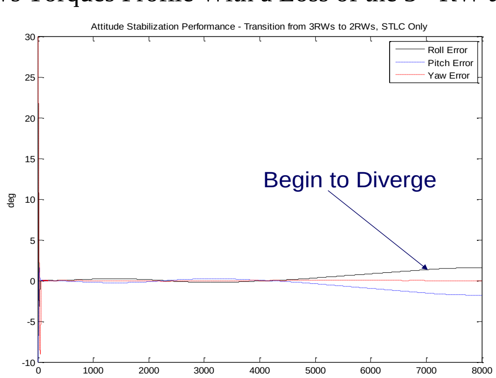

Figure 12: Degraded Attitude Pointing Accuracy Performance Due to Dynamic Transition, 3RWs to 2RWs

performance and mission life's extension beyond the traditional life span at GEO.

REFERENCES

[1] Q. M. Lam and I. Barkana, "Direct Adaptive Control Treatment to Loss of Attitude Control Actuators," Presented at *the AIAA GN&C August 2007, Hilton Head, SC*

[2] N.M. Horri and P.Palmer, Practical implementation of attitude-control algorithms for an underactuated satellite, J.Guid.ControlDyn.35(1) (2012)40–50.

[3] Haichao Gui, LeiJin and ShijieXu, "Attitude maneuver control of a two-wheeled spacecraft with bounded wheel speeds,"Acta Astronautica 88(2013)98–107, 2013 IAA. Published by Elsevier Ltd. All rights reserved.

[4] I. Barkana and H. Kaufman, Global stability and performance of a simplified adaptive algorithm, Int.J.Control 42(6) (1985) 1491–1505.

[5] I. Barkana, "Simple adaptive control – a stable direct model reference adaptive control methodology – brief survey," *Int. J. Adapt. Control Signal Process.* (2013)

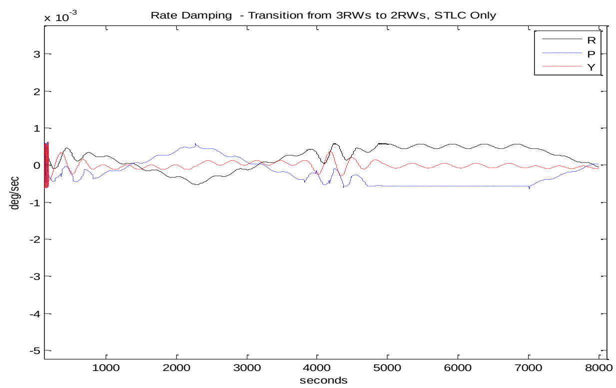

Figure 13: Degraded Rate Damping Performance Due to Dynamic Transition from 3RWs Down to 2RWs

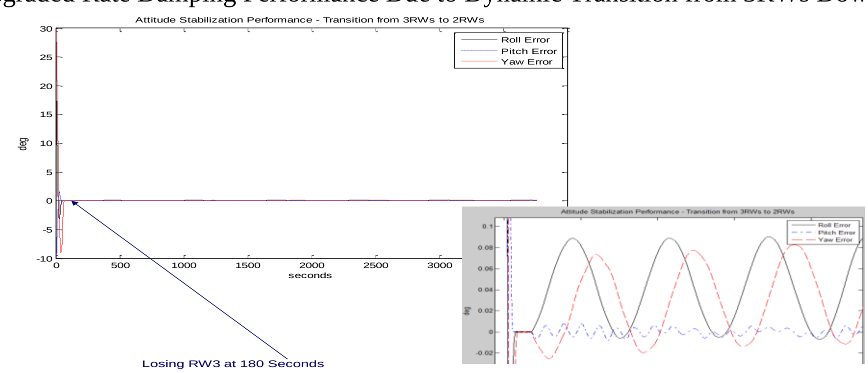

Figure 14: Attitude Pointing Performance Restoration Using the Joint STLC-DAC Control Laws

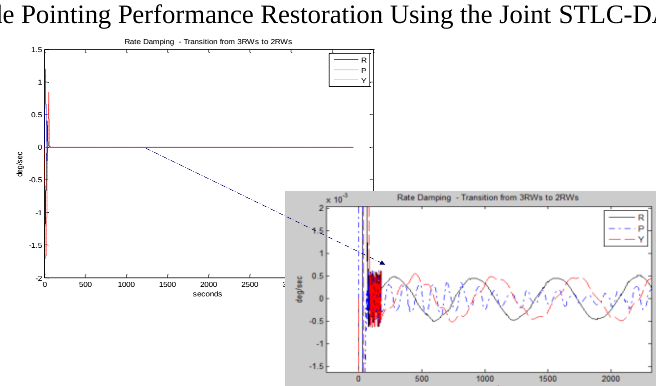

Figure 15: Rate Damping Performance Restoration Using the Joint STLC-DAC Control Laws